



**HAL**  
open science

## **VLITL is a major cross-beta-sheet signal for fibrinogen A alpha-chain frameshift variants**

Cyrille Garnier, Fatma Briki, Brigitte Nedelec, Patrick Le Pogamp, Ahmet Dogan, Nathalie Rioux-Leclercq, Renan Goude, Caroline Beugnet, Laurent Martin, Marc Delpech, et al.

### ► To cite this version:

Cyrille Garnier, Fatma Briki, Brigitte Nedelec, Patrick Le Pogamp, Ahmet Dogan, et al.. VLITL is a major cross-beta-sheet signal for fibrinogen A alpha-chain frameshift variants. *Blood*, 2017, 130 (25), pp.2799-2807. 10.1182/blood-2017-07-796185 . hal-01688181

**HAL Id: hal-01688181**

**<https://univ-rennes.hal.science/hal-01688181>**

Submitted on 24 Apr 2018

**HAL** is a multi-disciplinary open access archive for the deposit and dissemination of scientific research documents, whether they are published or not. The documents may come from teaching and research institutions in France or abroad, or from public or private research centers.

L'archive ouverte pluridisciplinaire **HAL**, est destinée au dépôt et à la diffusion de documents scientifiques de niveau recherche, publiés ou non, émanant des établissements d'enseignement et de recherche français ou étrangers, des laboratoires publics ou privés.

## **VLITL is a major cross- $\beta$ -sheet signal for fibrinogen A $\alpha$ -chain frameshift variants**

Cyrille Garnier,<sup>1,2</sup> Fatma Briki,<sup>3</sup> Brigitte Nedelec,<sup>4</sup> Patrick Le Pogamp,<sup>5</sup> Ahmet Dogan,<sup>6,7</sup> Nathalie Rioux-Leclercq,<sup>8</sup> Renan Goude,<sup>9</sup> Caroline Beugnet,<sup>10</sup> Laurent Martin,<sup>11</sup> Marc Delpech,<sup>12</sup> Frank Bridoux,<sup>13</sup> Gilles Grateau,<sup>14</sup> Jean Doucet,<sup>3</sup> Philippe Derreumaux,<sup>15</sup> Sophie Valleix<sup>4,10</sup>

<sup>1</sup> Université de Rennes 1, Campus de Beaulieu, 35042 Rennes, France. <sup>2</sup> Mécanismes Moléculaires dans les Démences Neurodégénératives Inserm U1198, Université Montpellier, Place Eugène Bataillon, 34095 Montpellier, France. <sup>3</sup> Laboratoire de Physique des Solides, Bât.510, Université Paris Sud F-91405 Orsay, France. <sup>4</sup> Institut National de la Santé et de la Recherche Médicale, Unité mixte de Recherche U\_1163, Institut IMAGINE, Université Paris Descartes, Sorbonne Paris Cité, 75015 Paris, France. <sup>5</sup> Service de Néphrologie, CHU de Rennes, 35042 Rennes, France. <sup>6</sup> Division of Anatomic Pathology, Mayo Clinic, Rochester, MN 55905. <sup>7</sup> Departments of Laboratory Medicine and Pathology, Memorial Sloan-Kettering Cancer Center, New York, NY 10065, USA. <sup>8</sup> Département d'Anatomie et Cytologie Pathologiques, Centre Hospitalo-Universitaire Pontchaillou, et CNRS/UMR6061, IFR140, Faculté de Médecine, Université de Rennes 1, 35042 Rennes, France. <sup>9</sup> Microbiologie risques infectieux, EA 1254 Université de Rennes 1, Campus de Beaulieu, 35042 Rennes cedex, France. <sup>10</sup> Laboratoire de Génétique Moléculaire, Hôpital Necker-Enfants Malades, 75015 Paris, Université Paris Descartes, Sorbonne Paris Cité, Faculté de Médecine Paris; AP-HP, Paris, France. <sup>11</sup> Service d'Anatomie Pathologique, Faculté de Médecine de Dijon, 21079 Dijon, France. <sup>12</sup> Laboratoire de Biochimie et Génétique Moléculaire, Hôpital Cochin, 75014 Paris, Université Paris Descartes, Sorbonne Paris Cité, Faculté de Médecine Paris; AP-HP. <sup>13</sup> Service de Néphrologie, CHU de Poitiers, et Centre national de référence des amyloses AL et autres maladies de dépôts d'immunoglobulines monoclonales, 86021 Poitiers, France. <sup>14</sup> Service de Médecine Interne, Hôpital Tenon, 75020 Paris, et Centre de référence des amyloses d'origine inflammatoire et de la fièvre méditerranéenne familiale; France. <sup>15</sup> Laboratoire de Biochimie Théorique, UPR9080 CNRS, Université Denis Diderot, Sorbonne Paris Cité, IBPC, Institut Universitaire de France, 75005 Paris, France.

**Short title:** VLITL is a major A $\alpha$ -chain fibril-forming motif

### **Key Points**

- VLITL is amyloid-prone and forms the ends of A $\alpha$ -chain fibrils *in vivo*.
- VLITL explains the molecular basis of A $\alpha$ -chain amyloidogenesis.

The first case of hereditary fibrinogen A $\alpha$ -chain amyloidosis was recognized more than 20 years ago, but disease mechanisms still remain unknown. Here we report detailed clinical and proteomics studies of a French kindred with a novel amyloidogenic fibrinogen A $\alpha$ -chain frameshift variant, Phe521Leufs, causing a severe familial form of renal amyloidosis. Next, we focused our investigations to elucidate the molecular basis that render this A $\alpha$ -chain variant amyloidogenic. We show that a 49-mer peptide derived from the C-terminal part of the Phe521Leufs-chain is deposited as fibrils in the patient's kidneys, establishing that only a small portion of Phe521Leufs directly contributes to amyloid formation *in vivo*. *In silico* analysis indicated that this 49-mer A $\alpha$ -chain peptide contained a motif (VLITL), with a high intrinsic propensity for  $\beta$ -aggregation at residues 44-48 of human renal fibrils. To experimentally verify the amyloid propensity of VLITL, we generated synthetic Phe521Leufs-derived peptides and compared their capacity for fibril formation *in vitro* with that of their VLITL-deleted counterparts. We show that VLITL forms typical amyloid fibrils *in vitro* and is a major signal for cross- $\beta$ -sheet self-association of the 49-mer Phe521Leufs-peptide identified *in vivo*, while its absence abrogates fibril formation. This study provides compelling evidence that VLITL confers amyloidogenic properties to A $\alpha$ -chain frameshift variants, yielding a previously unknown molecular basis for the pathogenesis of A $\alpha$ -chain amyloidosis.

## Introduction

Fibrinogen is a 340-kDa glycoprotein, composed of two identical heterotrimers, each consisting of one A $\alpha$ , one B $\beta$ , and one  $\gamma$ -chain.<sup>1</sup> Mutations altering any of these three chains are commonly associated with autosomal or recessive bleeding/thrombotic disorders (<http://site.geht.org/base-fibrinogene/>) without any clinical evidence of amyloidosis. However, a small fraction of A $\alpha$ -chain variants are amyloidogenic and lead to massive A $\alpha$ -chain deposition as amyloid fibrils in AFib-patient's kidneys. The first case of fibrinogen A $\alpha$ -chain-derived amyloidosis (AFib) has been described by Benson in 1993,<sup>2</sup> and until now, only the A $\alpha$ -chain has been linked to AFib (<http://amyloidosismutations.com/mut-afib.php>). AFib is a rare, late-onset, autosomal dominant condition characterized by massive amyloid deposition in the glomerular compartment of the kidney.<sup>2</sup> Heterozygous AFib-patients typically display a chronic kidney disease in the fourth/fifth decade of life leading to progressive end-stage renal failure.<sup>3</sup> Though amyloid mechanisms involved in AFib are still unknown, it was shown that AFib-fibrils were exclusively composed of the mutant A $\alpha$ -chain,<sup>2,4</sup> suggesting that the wild-type A $\alpha$ -chain does not contribute to amyloid deposition, analogous to what it was previously observed in patients with familial lysozyme,  $\beta_2$ -microglobulin, and apoC-III amyloidosis.<sup>5-7</sup> The therapeutic approach of AFib consists only in supportive treatment by dialysis and by renal or combined hepatorenal transplantation. Recently, Benson's group suggests that preemptive hepatic transplantation may avert the progression of renal damage and may be a promising treatment for AFib prior to the need for renal dialysis or kidney transplantation.<sup>8</sup> Although the first case of AFib was recognized more than 20 years ago, we still do not know which specific part of mutant A $\alpha$ -chain sequences directly participates in the  $\beta$ -aggregation process. To date, a total of 15 A $\alpha$ -chain variants are known to be amyloid-prone in humans, and remarkably these amyloidogenic variants are all clustered in a small portion of A $\alpha$ -chain from residues 517 to 555.<sup>2-4,9-13</sup> Missense A $\alpha$ -chain variants have been reported in several AFib-families worldwide, with Glu526Val being the most common amyloidogenic A $\alpha$ -chain variant.<sup>9</sup> In contrast, amyloidogenic A $\alpha$ -chain frameshift variants are "private" -ie that each of them has been reported in only a single family, and therefore available clinical information associated with these variants is very limited.<sup>3,4,10,12,13</sup> Two of them have

exceptionally been associated with pediatric AFib-cases,<sup>4,10</sup> suggesting that frameshifts may be particularly aggressive and likely highly prone to self-aggregation; therefore, it is of particular interest to investigate the precise mechanisms responsible for their amyloidogenicity.

We report a novel “private” amyloidogenic A $\alpha$ -chain frameshift variant (c.1620delT/Phe521Leufs) and show that renal fibrils of AFib patients are composed of a short polypeptide derived from the C-terminal part of the Phe521Leufs A $\alpha$ -chain without evidence of a wild-type counterpart. This additional confirmation of what part of the mutant A $\alpha$ -chain is deposited in the disease tissue of AFib-patients prompted us to explore how the mutant Phe521Leufs-chain contributes to A $\alpha$ -chain amyloid formation.

## **Materials and methods**

### **Genetic analysis**

Blood samples from the family members were obtained after their written informed consents. This study had the approval of the Ethics Committee of the Hospital of Rennes and was performed according to the Declaration of Helsinki. The entire coding region and flanking splice sites of exon 5 of *FGA* were sequenced as previously described.<sup>4</sup> The nomenclature of the fibrinogen A $\alpha$ -chain deletion is based on the *FGA* transcript reference (NM\_000508.3). For more clarity with the historically conventional nomenclature, the *FGA* variant is described as Phe521Leufs according to the mature protein without the signal peptide. According to the recommended Human Genome Variation Society (HGVS), which starts the amino acid numbering at the initiator methionine, Phe521Leufs corresponds to Phe540Leufs. In Table 1, all amyloidogenic A $\alpha$ -chain frameshift variants are listed with the two nomenclatures. To convert the conventional mature protein amino acid numbering to the HGVS nomenclature, add 19 nucleotides for A $\alpha$ -chain changes.

### **Histology and transmission electron microscopy of renal biopsies**

Renal biopsies were processed according to standard techniques, as previously described.<sup>4</sup> Immunostaining for the specific antibody (rabbit polyclonal antibody from Dr. Merrill Benson,

1:100) corresponding to the abnormal fibrinogen A $\alpha$ -chain (GAQNLASSQIQRN) was performed, as previously described.<sup>4</sup>

### **Laser microdissection and tandem mass spectrometry (LMD/MS) analysis**

The LMD and LC-MS/MS methods have been previously summarized in full text.<sup>14</sup>

### ***In silico* tools**

AMYPRED2 is a consensus algorithm for prediction of amyloidogenic determinants combining 11 different methods, available at <http://biophysics.biol.uoa.gr/AMYPRED2/>.<sup>15</sup> The cross- $\beta$  TANGO score results from a statistical mechanics model based on simple physico-chemical principles of secondary structure formation.<sup>16</sup> The PASTA energy is indicative of the aggregation propensity and predicts which portions of the sequence are more likely to stabilize the cross- $\beta$  core of fibrillar aggregates.<sup>17</sup>

### **Fibril formation**

All five synthetic peptides were purchased from genepep *prestation*, France, and stock solutions were prepared at the final concentration of 2 to 6 mM and stored at  $-20^{\circ}\text{C}$ . Fibril formation was induced in 10 mM MOPS buffer, 150mM NaCl, pH 7.2 at a final peptide concentration ranging from 0.125 to 1mM. Peptide solutions were incubated at room temperature without agitation or adjuvants from one day to two months.

### **Fluorescence experiments**

100 $\mu\text{L}$  of the five peptides were added to 900  $\mu\text{L}$  of fibrillation buffer containing Thioflavin T (5  $\mu\text{M}$  final concentration). Fluorescence was measured with a Perkin-Elmer Luminescence Spectrometer LS55 with slit widths of 10 nm. The excitation was at 450 nm and emission spectra of ThT were recorded from 470 to 600 nm.

### **Transmission electron microscopy of aggregates formed *in vitro***

Aliquot of the five peptides (10  $\mu\text{l}$  with a concentration of  $\sim 10\text{mg/ml}$ ) were placed on carbon-coated copper grids (300 mesh), washed and negatively stained for 1min with 1% (wt/vol) uranyl acetate, and wicked dry prior to analysis using a Philips CM12 transmission electron microscope operating at accelerating voltages of 120 kV.

### **X-ray microdiffraction experiments performed on *in vitro* aggregate samples and on *ex vivo* renal fibrils**

All samples were pelleted by centrifugation at 5000g for 10 min. Small concentrated drops of samples were deposited on cylindrical fibres of about 100 $\mu$ m diameter. X-ray microdiffraction was performed at the ESRF-European Synchrotron Radiation Facility (Grenoble, France) on the microfocus beam line ID13, as previously described.<sup>18</sup>

## **Results**

### **Phe521Leufs is a novel amyloidogenic « private » frameshift variant of fibrinogen A $\alpha$ -chain associated with a severe form of renal amyloidosis**

Amyloidosis was initially diagnosed from a 27-year-old woman (patient I.1) who presented proteinuria (1.30 g/L) during routine medical screening at her first pregnancy (Figure 1A). Progressively, she developed nephrotic syndrome without hypertension (120/80 mmHg). On physical examination, she had no signs of peripheral or autonomic neuropathy, and all cardiac investigations were normal. A renal biopsy was performed and amyloidosis was diagnosed, but the etiology of her renal amyloidosis remained undetermined. Three years later, this patient was diagnosed with malignant hypertension (210/130 mmHg), and was treated with transfusion of fresh frozen plasma and association of several anti-hypertensive drugs, resulting in adequate control of blood pressure. However, she continued to develop uremia leading to acute renal failure requiring hemodialysis. One year later, she underwent her first renal transplantation, but amyloidosis recurred on the renal graft five years later, and she received her second renal graft. The etiology of this renal amyloidosis was reevaluated when one of her daughter (II.2) began to manifest proteinuria at 22-years old associated with glomerular amyloid deposits. This proband's daughter also developed an acute episode of malignant hypertension leading to acute renal failure and hemodialysis. In both of these affected AFib-probands, there was no history of bleeding or thrombotic disorders (even during surgical procedures and during the nephrotic phase), and all routine coagulation investigations were normal including Clauss fibrinogen activity level, fibrinogen antigen level, activated partial thromboplastin time, prothrombin time, thrombin time, and

reptilase time, indicating absence of significant quantitative or qualitative fibrin clot abnormalities. Finally, hereditary AFib was confirmed on the basis of history of renal disease in two family members, documented evidence of renal dysfunction secondary to Congo red amyloid deposits in glomeruli, histological evidence of amyloid fibrils at electron microscopy, immunohistochemistry of renal biopsies, and detection of *FGA* mutation (Figures 1A-E). The two AFib-probands (I.1 and II.2) were heterozygous for a novel single base pair deletion (c.1620delT), expected to alter the reading frame of the A $\alpha$ -chain mRNA at codon 521: Phe521Leufs (numbering according to the mature protein) or Phe540Leufs (according to the recommended HGVS nomenclature, including the signal peptide). This mutation was not detected in family members II.1 and II.3 who had no proteinuria, confirming that this novel A $\alpha$ -chain variant segregated with renal disease in this kindred (Figures 1A and 1E). This thymine deletion is expected to cause loss of the last C-terminal 62 amino acids of the wild-type A $\alpha$ -chain and, instead, the incorporation of 27 new residues (521-LSVRLSLGAQNLASSQIQRNPVLITLG-547) before premature termination of the translation at codon 548 (Figure 1D and Figure 2B). Therefore, the genetic data were concordant with immunohistochemistry analysis showing that the Congo red glomeruli deposits positively stained with a specific anti-human A $\alpha$ -chain monoclonal antibody that recognized the mutant C-terminal portion of all amyloidogenic frameshifts (Figure 1D).<sup>4</sup> Sequence alignment of Phe521Leufs with amyloidogenic A $\alpha$ -chain frameshift variants reported thus far showed that all invariably truncate at codon 548, producing highly similar mutant C-terminal sequences with a common portion of 15 amino acids, ASSQIQRNPVLITLG, residues 533-547 (Table 1).

### **The C-terminus end of Phe521Leufs chain constitutes amyloid fibrils *in vivo***

To determine which part of the A $\alpha$ -chain contributes to the formation of amyloid fibrils, renal deposits from proband II.2 were extracted by laser-microdissection/liquid chromatography and tandem mass spectrometry (LMD/MS),<sup>14</sup> and the Phe521Leufs amyloid proteome was compared to the proteome obtained from AFib patients carrying the Glu526Val missense variant, the most common amyloidogenic A $\alpha$ -chain variant. Several independent samples (replicates) were analyzed for Phe521Leufs and Glu526Val variants. For both variants, the amyloid proteome profile indicated that A $\alpha$ -

chain showed the highest probability score in the deposits and the signature proteins (SAP and apoE) were present, giving confidence in the identification of amyloid (Figure 2A). Peptides corresponding to the new C-terminal sequence of Phe521Leufs were detected only in the case carrying this mutation and not in Glu526Val cases (Figure 2A). Detailed examination of the protein coverage of Phe521Leufs showed that the amyloid peptide contained all of the modified C-terminal sequence encoded by the Phe521Leufs allele (100% coverage) but not the wild-type C-terminal A $\alpha$ -chain sequence after residue 521 (Figure 2B). In conclusion, the amyloid peptide characterized in Phe521Leufs deposits was a hybrid 49-mer fragment with the first 22 residues identical to the wild-type A $\alpha$ -chain residues 499-520 (AFFDTASTGKTFPGFFSPMLGE), and the C-terminal 27 residues corresponding to the sequence encoded by Phe521Leufs (LSVRLSLGAQNLASSQIQRNPVLITLG) (Figure 2B). Therefore, our amyloid proteome analysis indicated that wild-type A $\alpha$ -chain does not contribute to amyloid formation, and that only the C-terminal sequence generated by the Phe521Leufs allele is amyloid *in vivo*, a finding consistent with previous publications.<sup>2,4,13</sup>

### **VLITL is predicted to be a major cross- $\beta$ -sheet signal of Phe521Leufs chain**

To explore why the mutant Phe521Leufs sequence contributes to amyloid formation, we first performed *in silico* analyses on the full-length sequences of Phe521Leufs and all frameshifts to search for motifs with a propensity to form amyloid (Table 1).<sup>19,20</sup> We used AMYLPRED2,<sup>15</sup> which combines 11 individual algorithms, and PASTA2,<sup>17</sup> which predicts which amino acid and  $\beta$ -sheet orientation is energetically favored. Combined algorithms indicated that, in all cases, the amino acid sequence encoded by each amyloidogenic frameshift variant created a common short stretch motif with high amyloidogenic propensity that involved a five-residue fragment (VLITL) (Figures 3A and 3B). TANGO identified VLITL as the unique hot-spot with a high intrinsic propensity for  $\beta$ -aggregation regardless of pH and ionic strength (Figure 3A), and PASTA2 predicted that VLITL forms parallel in-register intermolecular  $\beta$ -sheets in amyloid (favorable pairing energy of -5.57, corresponding to 10.7 kcal/mol) (Figure 3B). Consistent with these predictions, VLITL is consistently present in A $\alpha$ -chain frameshift variants associated with renal amyloidosis (Table 1), while VLITL is absent from the amino acid sequences of those that are not clinically amyloidogenic (<http://site.geht.org/base-fibrinogene/>).<sup>21,22</sup> This genotype-phenotype relationship suggests that nucleotide

indel mutations producing mutant A $\alpha$ -chains containing VLITL at their C-termini will be likely amyloidogenic (Table 1). More importantly, we show here that VLITL is part of renal fibrils of AFib-patient II.2 (residues 44-48 of the 49-mer amyloid peptide found *ex vivo*) (Figure 2B), reinforcing the view that VLITL indeed might confer amyloidogenic properties.

### **VLITL responsible for the amyloidogenic property of Phe521Leufs-derived peptides**

To experimentally verify that VLITL is the major amyloid sequence determinant of A $\alpha$ -chain frameshifts, we generated synthetic A $\alpha$ -chain derived-peptides containing the predicted amyloid-prone VLITL motif, and compared their capacity for fibril formation with that of their VLITL-deleted counterparts. To this end, we designed AFFDTASTGKTFPGFFSPMLGELSVRLSLGAQNLASSQIQRNPVLITLG, the 49-mer full-length Phe521Leufs-peptide identified in AFib-patient's deposits, and its corresponding VLITL-deleted control (AFFDTASTGKTFPGFFSPMLGELSVRLSLGAQNLASSQIQRNP\_G). We also investigated the amyloid propensity of the ASSQIQRNPVLITLG-peptide, common to all amyloidogenic A $\alpha$ -chain variants, and its VLITL-deleted counterpart ASSQIQRNP\_G. Fibrillogenesis experiments were performed under the same physiological conditions and amyloid formation evaluated using ThT, a dye binding to  $\beta$ -sheet aggregates with a characteristic maximum emission fluorescence intensity at 485 nm, TEM to determine the morphological features of aggregates, and X-ray microdiffraction (XRD) to ensure that aggregates possess the typical cross- $\beta$  architecture.<sup>23,24</sup> As shown in Figures 4A-D, AFFDTASTGKTFPGFFSPMLGELSVRLSLGAQNLASSQIQRNPVLITLG self-assembled into ThT-positive,  $\beta$ -sheet-enriched fibrillar aggregates exhibiting cross- $\beta$  architecture that unambiguously define amyloid fibrils. The ThT profile for AFFDTASTGKTFPGFFSPMLGELSVRLSLGAQNLASSQIQRNP\_G did not parallel that obtained for its corresponding amyloid VLITL-counterpart. Despite a mild fluorescence intensity, maximum emission was observed at 510 nm instead of 485 nm, indicating that these aggregates have distinct dye-binding characteristics from typical amyloid fibrils (Figure 4A). Such a ThT profile has been associated with unstructured/amorphous aggregates.<sup>25</sup> Consistent with ThT assay, TEM of

AFFDTASTGKTFPGFFSPMLGELSVRLSLGAQNASSQIQRNP<sub>G</sub> revealed spherical species that are distinguishable from the fibrillar morphology of aggregates formed by AFFDTASTGKTFPGFFSPMLGELSVRLSLGAQNASSQIQRNPVLITLG (Figure 4B and Figure 5A). Even after an extended incubation period, AFFDTASTGKTFPGFFSPMLGELSVRLSLGAQNASSQIQRNP<sub>G</sub> assembled into small spherical species without formation of fibrils (Figure 5A). In contrast, AFFDTASTGKTFPGFFSPMLGELSVRLSLGAQNASSQIQRNPVLITLG organized into fibrils with a diameter of  $11.4 \pm 0.9$  nm and twisted ribbon-like substructure (Figure 4B). XRD of AFFDTASTGKTFPGFFSPMLGELSVRLSLGAQNASSQIQRNPVLITLG-fibrils showed a typical “cross- $\beta$ ” molecular architecture with 4.72 Å sharp signal arising from the repeated  $\beta$ -strand spacing along the fibril axis and 11.5 Å signal corresponding to the stacking of  $\beta$ -sheets perpendicular to the fibril axis (Figures 4C and 4D). In contrast, XRD pattern of AFFDTASTGKTFPGFFSPMLGELSVRLSLGAQNASSQIQRNP<sub>G</sub> showed one diffuse reflection ring around 4.5 Å arising from the mean distance of randomly distributed peptide chains (Figure 5B). Therefore, XRD provided definitive structural evidence that species formed by AFFDTASTGKTFPGFFSPMLGELSVRLSLGAQNASSQIQRNP<sub>G</sub> lack ordered cross- $\beta$  organization, the major diagnostic hallmark of amyloid. Experimental studies of ASSQIQRNPVLITLG demonstrated that this VLITL-containing peptide bound ThT with a characteristic amyloid maximum emission fluorescence intensity at 485 nm and formed fibrillar aggregates with a diameter of  $13 \pm 0.9$  nm and cross- $\beta$  molecular architecture (Figures 4E-G). In contrast, ASSQIQRNP<sub>G</sub>, did not exhibit any ThT spectral change (Figure 4E), and did not form aggregates (amorphous or fibrillar in nature) (data not shown), demonstrating that ASSQIQRNP<sub>G</sub> does not form any kind of amyloid species under the same physiological conditions that the ASSQIQRNPVLITLG-peptide does. Therefore, our experiments show that the 49-mer and 15-mer Phe521Leufs-derived peptides are readily amyloidogenic *in vitro* but lose their fibril-forming ability when VLITL is absent, supporting that their amyloidogenic behavior depends on VLITL amyloidogenic properties. Next, we experimentally verified whether VLITL itself forms amyloid *in vitro*. A ThT assay of VLITL showed typical amyloid enhancement of fluorescence emission at 485 nm (Figure 4I). In addition, TEM revealed twisted mature

fibrils with a ribbon-like appearance (Figures 4J and 4K) and XRD confirmed that VLITL-fibrils are amyloid with a highly ordered and well-defined cross- $\beta$  structure (Figure 4L).

### **Structural similarities between *in vitro* and *ex vivo* Phe521Leufs-derived fibrils**

The structures of Phe521Leufs-derived fibrils generated *in vitro* were compared to those formed in AFib-patient kidneys (individual II.2). To this end, we performed *ex situ* XRD studies of Phe521Leufs-fibrils using kidney cuts obtained without denaturing extraction procedures to preserve the natural state of aggregates formed *in vivo*, offering the opportunity to gain structural information on fibrils in their natural cellular context (Figure 3H).<sup>18</sup> XRD showed that the signal of the equatorial reflection from natural fibrils was very close to that of fibrils generated by ASSQIQRNPVLITLG, recapitulating the structural features of renal AFib-fibrils in physiological conditions (Figures 4C, 4G, 4H, and 4L).<sup>26</sup> Therefore, this mutant 15-mer A $\alpha$ -chain derived-sequence likely governs the detailed structure of Phe521Leufs-fibrils formed in patient kidneys, and might constitute a valuable “minimalist” *in vitro* amyloid model.

## **Discussion**

Here, in addition to report a new “private” A $\alpha$ -chain amyloidogenic frameshift variant, the aim of this study was to focus on the molecular mechanisms by which fibrinogen A $\alpha$ -chain frameshift variants become amyloidogenic in humans.

Our results show that VLITL is a key amyloid-prone motif located at the C-terminally mutant end of all A $\alpha$ -chain frameshift sequences, conferring amyloidogenic properties to A $\alpha$ -chain frameshift variants. In this study, we first characterized which part of the A $\alpha$ -chain was deposited in Phe521Leufs-patient’s tissues, and we demonstrated that a short 49-mer peptide deriving from the Phe521Leufs-allele formed the renal fibrils. These clinico-anatomopathological findings overlap those obtained from our French AFib-kindred carrying the Val522Alafs variant which had previously documented that a 49-amino acid peptide encoded by the Val522Alafs-allele was similarly deposited as fibrils in kidneys.<sup>4</sup> More recently, Yazaki et al. also confirmed that the carboxyl terminal region of the amyloidogenic Ser523Argfs variant, containing

VLITL, constituted AFib-patient's renal deposits.<sup>13</sup> Therefore, three *ex vivo* biochemical analysis of amyloid deposits from AFib-patient's carrying three distinct frameshift variants of A $\alpha$ -chain concordantly established that only the C-terminal fragments of A $\alpha$ -chain frameshift variants contribute to amyloid formation, and not the wild-type A $\alpha$ -chain. We then tested the hypothesis that these highly similar A $\alpha$ -chain C-terminal mutant sequences, specific to amyloidogenic variants, might contain segments with a high propensity to self-aggregate into  $\beta$ -sheets rendering mutant A $\alpha$ -chains amyloidogenic. Our *in silico* analysis predicted that the C-terminal end of all mutant A $\alpha$ -chains contained a major amyloid hot spot, VLITL. This prediction was in good concordance with the fact that VLITL was found within renal amyloid deposits of Phe521Leufs-, Val522Alafs- and Ser523Argfs-AFib patients.<sup>4,13</sup> To experimentally verify that VLITL is a major  $\beta$ -sheet signal of A $\alpha$ -chain frameshift variants, we evaluated the ability of synthetic Phe521Leufs-derived peptides containing the VLITL motif to polymerize into  $\beta$ -sheet *in vitro*. We also compared their capacity for fibril formation with that of their VLITL-deleted counterparts. We provide *in vitro* evidence that VLITL is a fibril-forming motif, necessary for the  $\beta$ -sheet arrangement of the full-length A $\alpha$ -chain peptide deposited as extracellular fibrils in Phe521Leufs-patient's kidneys, while its absence abrogates fibril formation of Phe521Leufs-derived peptides. Therefore, combined *in vitro* and *in vivo* experiments support that the amyloidogenic behavior of the Phe521Leufs variant depends on the amyloidogenic properties of VLITL. The location of VLITL at the extreme end of renal fibrils probably renders this motif easily accessible for intermolecular interactions *in vivo*. VLITL satisfies two major criteria that are recognized as essential for triggering amyloid formation: high  $\beta$ -sheet propensity and appropriate position within the mutant A $\alpha$ -chains for nucleating fibril formation.<sup>27,28</sup> It is important to note that Phe521Leufs-derived peptides form amyloid fibrils in "physiological" experimental conditions. On this basis, it was therefore particularly relevant to compare the structural characteristics of Phe521Leufs-derived fibrils formed *in vitro* with those formed in the Phe521fs-patient's kidneys. To this end, X-ray analysis of A $\alpha$ -chain-fibrils from Phe521fs-patients was performed "*in situ*", directly on the pathological renal tissue without denaturing extraction procedures, to preserve the natural state of A $\alpha$ -chain aggregates.<sup>18</sup> This structural analysis revealed that ASSQIQRNPVLITLG-fibrils closely reproduced the  $\beta$ -sheet structural organization of A $\alpha$ -

chain-fibrils assembled in their natural cellular context. Therefore, ASSQIQRNPVLITLG, the mutant portion common to all amyloidogenic frameshifts, is a “minimalist” *in vitro* A $\alpha$ -chain model suitable for all amyloidogenic A $\alpha$ -chain frameshift variants. This *in vitro* A $\alpha$ -chain model might be useful for testing anti-amyloid agents targeting the VLITL motif because we showed that deleting VLITL disrupts fibril aggregation propensity of synthetic Phe521Leufs-derived peptides. Also, this *in vitro* model can be useful to conduct high-resolution structure investigations to shed light on the precise atomistic structure of A $\alpha$ -chain frameshift derived-fibrils.

The reasons why fragments of the mutant A $\alpha$ -chain C-terminus accumulate and form amyloid in kidneys, and why the mutant A $\alpha$ -chain could not be detected in the plasma of AFib-patients are not understood,<sup>4</sup> but it has been proposed that it can be the consequence of an accelerated metabolism of the mutant A $\alpha$ -chain.<sup>4</sup> In case of A $\alpha$ -chain dysfibrinogenic variants, experiments carried on the His494fs and Ala499fs frameshift variants, each introducing in their mutant C-terminal part a novel unpaired cysteine residue, revealed that these mutant A $\alpha$ -chains circulated as disulphide-linked complexes with albumin. More importantly, it has been shown that these abnormal A $\alpha$ -chain-albumin complexes directly altered the fibrin clot structure, conferring to the patients a dysfibrinogenic phenotype, clinically apparent as recurrent episodes of thromboembolism.<sup>21,22,29</sup> Unlike A $\alpha$ -chain dysfibrinogenic variants, the amino acid composition of the mutant C-terminus of amyloidogenic frameshift variants do not contain a novel cysteine residue, thus they are unlikely able to form abnormal disulphide conjugates with albumin. This could explain why, despite lacking Lys556, Lys580, and Lys601 in the  $\alpha$ C-domain important for factor XIII cross-linking, AFib-patients do not show clinical and biological evidence of clotting disorders. Further, we can speculate that these “albumin-free” amyloidogenic A $\alpha$ -chains might be more susceptible to undergo an aberrant proteolytic cleavage, yielding high concentrations of a catabolic intermediate containing the amyloid-prone VLITL motif serving as an amyloid core to initiate fibrillogenesis in the cellular environment of the kidney. Consistent with data from the literature, it is unlikely a coincidence that no mutations involving a cysteine residue in the A $\alpha$ -chain have been associated with AFib, while they explain a large number of congenital dysfibrinogenemias associated with circulating fibrinogen-albumin conjugates (<http://site.geht.org/base-fibrinogene/>). An instructive

example is given by Fibrinogen Dusart, caused by the replacement of arginine 554 by cysteine (Arg554Cys) in the A $\alpha$ -chain, which is associated with A $\alpha$ -chains-554C-albumin complexes and recurrent episodes of thrombosis,<sup>30,31</sup> while replacement of Arg554 by leucine (Arg554Leu) causes renal AFib-amyloidosis.<sup>2</sup> The six polypeptide chains of the normal fibrinogen molecule are covalently linked by numerous interchain disulphide bonds, with no free sulphhydryl groups,<sup>1</sup> supporting that an unpaired cysteine residue in the fibrinogen molecule might be critical on overall clot structure.

In summary, we provide compelling evidence that VLITL is part of Phe521Leufs-fibrils formed *in vivo*, and is a major fibril-forming motif necessary for  $\beta$ -sheet arrangement of the full-length A $\alpha$ -chain Phe521Leufs-peptide identified in AFib-patient's kidneys. This VLITL amyloid motif, exclusively present at the C-terminal end of amyloidogenic A $\alpha$ -chain frameshift sequences, and also previously identified in amyloid deposits of Val522Alafs and Ser523Argfs AFib-patients support that VLITL is predictive of high risk of A $\alpha$ -chain amyloid formation. This finding sheds light on the as yet unresolved issue of the mechanisms underlying A $\alpha$ -chain amyloidogenesis, yielding an uncommon example among hereditary amyloidoses.

## Acknowledgments

We thank all of the family members for their participation in this study, and l'Association Française contre l'Amylose. We thank Fabrice Senger and Marie-Paule Ramée for technical assistance with light microscopy and transmission electron microscopy, respectively. We thank Céline Leroux for her assistance with *FGA* sequencing, and J D Theis for his assistance in proteomics analysis at the Mayo Clinic.

This work was supported in part by grants from l'Association Française contre l'Amylose.

## Authorship

Contribution: P.L-P collected the blood samples of the family, interpreted the clinical data, and supervised histology and immunohistochemistry analysis. C.G and R.G

performed and analyzed the *in vitro* fibrillogenesis studies. F.B and J.D performed and analyzed the X-ray diffraction studies. N.R-L and L.M performed and analyzed the microscopy and immunohistochemical analysis. A.D, J.T, and J.A performed the LMD/MS analysis. C.B performed the molecular screening. F.B, M.D contributed to the discussion of the data. G.G contributed to the discussion, provided critical review of the manuscript, edited and approved the final version of the manuscript. B.N contributed to the preparation of the manuscript and prepared the figures. P.D, S.V analyzed *in silico* calculations and designed *in vitro* experiments. S.V supervised all aspects of this work, developed the whole idea, designed the experiments, collected and interpreted the data and wrote the manuscript.

Conflict-of-interest disclosure: The authors declare no competing interests.

Correspondence: Pr. Sophie Valleix, Laboratoire de Génétique Moléculaire, Hôpital Necker-Enfants Malades, 75015 Paris, Université Paris Descartes, Sorbonne Paris Cité, Faculté de Médecine Paris; AP-HP, Paris, France. E-mail : [sophie.valleix@aphp.fr](mailto:sophie.valleix@aphp.fr)

## References

1. Weisel JW, Litvinov RI. Mechanisms of fibrin polymerization and clinical implications. *Blood*. 2013;121(10):1712–1719.
2. Benson MD, Liepnieks J, Uemichi T, Wheeler G, Correa R. Hereditary renal amyloidosis associated with a mutant fibrinogen alpha-chain. *Nat. Genet.* 1993;3(3):252–255.
3. Gillmore JD, Lachmann HJ, Rowczenio D, et al. Diagnosis, pathogenesis, treatment, and prognosis of hereditary fibrinogen A alpha-chain amyloidosis. *J. Am. Soc. Nephrol. JASN.* 2009;20(2):444–451.
4. Hamidi Asl L, Liepnieks JJ, Uemichi T, et al. Renal amyloidosis with a frame shift mutation in fibrinogen aalpha-chain gene producing a novel amyloid protein. *Blood*. 1997;90(12):4799–4805.
5. Valleix S, Verona G, Jourde-Chiche N, et al. D25V apolipoprotein C-III variant causes dominant hereditary systemic amyloidosis and confers cardiovascular protective lipoprotein profile. *Nat. Commun.* 2016;7:10353.
6. Valleix S, Gillmore JD, Bridoux F, et al. Hereditary systemic amyloidosis due to Asp76Asn variant  $\beta$ 2-microglobulin. *N. Engl. J. Med.* 2012;366(24):2276–2283.
7. Pepys MB, Hawkins PN, Booth DR, et al. Human lysozyme gene mutations cause hereditary systemic amyloidosis. *Nature*. 1993;362(6420):553–557.
8. Fix OK, Stock PG, Lee BK, Benson MD. Liver transplant alone without kidney transplant for fibrinogen A $\alpha$ -chain (AFib) renal amyloidosis. *Amyloid Int. J. Exp. Clin. Investig. Off. J. Int. Soc. Amyloidosis.* 2016;23(2):132–133.

9. Rowczenio DM, Noor I, Gillmore JD, et al. Online registry for mutations in hereditary amyloidosis including nomenclature recommendations. *Hum. Mutat.* 2014;35(9):E2403-2412.
10. Kang HG, Bybee A, Ha IS, et al. Hereditary amyloidosis in early childhood associated with a novel insertion-deletion (indel) in the fibrinogen Aalpha chain gene. *Kidney Int.* 2005;68(5):1994-1998.
11. Uemichi T, Liepnieks JJ, Benson MD. Hereditary renal amyloidosis with a novel variant fibrinogen. *J. Clin. Invest.* 1994;93(2):731-736.
12. Uemichi T, Liepnieks JJ, Yamada T, et al. A frame shift mutation in the fibrinogen A alpha chain gene in a kindred with renal amyloidosis. *Blood.* 1996;87(10):4197-4203.
13. Yazaki M, Yoshinaga T, Sekijima Y, et al. The first pure form of Ostertag-type amyloidosis in Japan: a sporadic case of hereditary fibrinogen A $\alpha$ -chain amyloidosis associated with a novel frameshift variant. *Amyloid Int. J. Exp. Clin. Investig. Off. J. Int. Soc. Amyloidosis.* 2015;22(2):142-144.
14. Sethi S, Vrana JA, Theis JD, et al. Laser microdissection and mass spectrometry-based proteomics aids the diagnosis and typing of renal amyloidosis. *Kidney Int.* 2012;82(2):226-234.
15. Tsolis AC, Papandreou NC, Iconomidou VA, Hamodrakas SJ. A consensus method for the prediction of "aggregation-prone" peptides in globular proteins. *PLoS One.* 2013;8(1):e54175.
16. Fernandez-Escamilla A-M, Rousseau F, Schymkowitz J, Serrano L. Prediction of sequence-dependent and mutational effects on the aggregation of peptides and proteins. *Nat. Biotechnol.* 2004;22(10):1302-1306.
17. Walsh I, Seno F, Tosatto SCE, Trovato A. PASTA 2.0: an improved server for protein aggregation prediction. *Nucleic Acids Res.* 2014;42(Web Server issue):W301-307.
18. Briki F, Vérine J, Doucet J, et al. Synchrotron x-ray microdiffraction reveals intrinsic structural features of amyloid deposits in situ. *Biophys. J.* 2011;101(2):486-493.
19. Ventura S, Zurdo J, Narayanan S, et al. Short amino acid stretches can mediate amyloid formation in globular proteins: the Src homology 3 (SH3) case. *Proc. Natl. Acad. Sci. U. S. A.* 2004;101(19):7258-7263.
20. Yoon S, Welsh WJ. Detecting hidden sequence propensity for amyloid fibril formation. *Protein Sci. Publ. Protein Soc.* 2004;13(8):2149-2160.
21. Homer VM, Mullin JL, Brennan SO, Barr A, George PM. Novel Aalpha chain truncation (fibrinogen Perth) resulting in low expression and impaired fibrinogen polymerization. *J. Thromb. Haemost. JTH.* 2003;1(6):1245-1250.
22. Margaglione M, Vecchione G, Santacroce R, et al. A frameshift mutation in the human fibrinogen Aalpha-chain gene (Aalpha(499)Ala frameshift stop) leading to dysfibrinogen San Giovanni Rotondo. *Thromb. Haemost.* 2001;86(6):1483-1488.
23. Makin OS, Sikorski P, Serpell LC. Diffraction to study protein and peptide assemblies. *Curr. Opin. Chem. Biol.* 2006;10(5):417-422.
24. Nilsson MR. Techniques to study amyloid fibril formation in vitro. *Methods San Diego Calif.* 2004;34(1):151-160.
25. Mothi N, Muthu SA, Kale A, Ahmad B. Curcumin promotes fibril formation in F isomer of human serum albumin via amorphous aggregation. *Biophys. Chem.* 2015;207:30-39.
26. Riek R, Eisenberg DS. The activities of amyloids from a structural perspective. *Nature.* 2016;539(7628):227-235.
27. Esteras-Chopo A, Serrano L, López de la Paz M. The amyloid stretch hypothesis: recruiting proteins toward the dark side. *Proc. Natl. Acad. Sci. U. S. A.* 2005;102(46):16672-16677.
28. Pastor MT, Esteras-Chopo A, Serrano L. Hacking the code of amyloid formation: the amyloid stretch hypothesis. *Prion.* 2007;1(1):9-14.
29. Dempfle C-E, George PM, Borggrefe M, Neumaier M, Brennan SO. Demonstration of heterodimeric fibrinogen molecules partially conjugated with albumin in a novel dysfibrinogen: fibrinogen Mannheim V. *Thromb. Haemost.* 2009;102(1):29-34.

30. Koopman J, Haverkate F, Grimbergen J, et al. Molecular basis for fibrinogen Dusart (A alpha 554 Arg-->Cys) and its association with abnormal fibrin polymerization and thrombophilia. *J. Clin. Invest.* 1993;91(4):1637-1643.
31. Mosesson MW, Siebenlist KR, Hainfeld J f, et al. The relationship between the fibrinogen D domain self-association/cross-linking site (gammaXL) and the fibrinogen Dusart abnormality (Aalpha R554C- $\alpha$ 1): clues to thrombophilia in the "Dusart syndrome." *J. Clin. Invest.* 1996;97(10):2342-2350.

**Table 1**

A $\alpha$ -chain frameshift variants associated with renal amyloidosis	FGA nucleotide variations	Predicted C-terminal mutant A $\alpha$ -chains encoded by the respective shifted reading frames with premature stop at codon 548	Renal A $\alpha$ -chain fibril composition
<b>Met517_Phe521 delinsGlnSerfs*28</b> (p. Met536_Phe540delinsGlnSerfs*28 (Kang et al., Kidney Int 2005))	c.1606_1620 delATGTTAGGAGAGTTT insCA	... <b>QSVRLSLGAQNLASSQIQRN</b> <u>PVLITLG</u>	No
<b>Phe521Leufs*28</b> (p.Phe540Leufs*28) (New variant reported here)	c.1620delT	... <b>LSVRLSLGAQNLASSQIQRN</b> <u>PVLITLG</u>	Yes (This report)
<b>Phe521Serfs*27</b> (p.Phe540Ser*27) (The XVth ISA)	c.1619_1622delTTGT	... <b>SVRLSLGAQNLASSQIQRN</b> <u>PVLITLG</u>	Yes
<b>Val522Alafs*27</b> (p.Val541Alafs*27) (Hamidi et al., Blood 1997)	c.1622delT	... <b>AVRLSLGAQNLASSQIQRN</b> <u>PVLITLG</u>	Yes (Our previous AFib-kindred)
<b>Ser523Argfs*26</b> (p.Ser543Argfs*26) (Yazaki et al., Amyloid 2015)	c.1624_1627del AGTG	... <b>RLSLGAQNLASSQIQRN</b> <u>PVLITLG</u>	Yes
<b>Glu524Glufs*25</b> (p.Glu543Glufs*25) (Uemichi et al., Blood 1996)	c.1629delG	... <b>LSLGAQNLASSQIQRN</b> <u>PVLITLG</u>	No
<b>Thr525Thrfs*24</b> (p.Thr544Thrfs*24) (Gillmore et al., J Am Soc Nephrol 2009)	c.1632delT	... <b>SLGAQNLASSQIQRN</b> <u>PVLITLG</u>	Yes
<b>Ser532Serfs*16</b> (p.Ser551Serfs*16) (The XIIIth ISA)	c.1653delT	... <b>ASSQIQRN</b> <u>PVLITLG</u>	No

## Figure legends

**Figure 1. Novel amyloidogenic“private” A $\alpha$ -chain frameshift variant in a French family.** (A) shows the family pedigree of the AFib-kindred with familial segregation of the Phe521Leufs variant due to a single thymine deletion at Phe521. Squares denote male family members, circles female family members, and solid symbols affected family members. (B) shows partial sequence of *FGA* exon 5 from II.2, indicating heterozygosity for deletion of a single thymine leading to superimposed sequences after codon 521. (C) shows Congo red deposits in the glomeruli of renal specimens from II.2 (x400). (D) illustrates the amyloid fibrils found in the mesangium and under the glomerular basement membrane, appearing as straight unbranched fibrils with 10 nm diameter by EM (x1400). (E) shows positive staining with the specific A $\alpha$ -chain antibody raised against the C-terminal A $\alpha$ -chain mutant sequence (black arrow).

**Figure 2. The C-terminal mutant region predicted by Phe521Leufs is detected in renal amyloid deposits, but not its wild-type counterpart.** (A) shows the results of LMD/MS-based proteomics analysis of amyloid plaques from seven cases of AFib. Cases 1-6 carry the A $\alpha$ -chain Glu526Val (E526V) variant and case 7 the Phe521Leufs (F521fs) variant. The identified proteins are listed by relative probability score for identity, and the top 20 proteins of 103 proteins are shown. The columns show the protein name, the UniProt identifier (protein accession number in the UniProt database, <http://www.uniprot.org/>), the molecular weight of the protein, and one microdissection from 7 patient specimens involved by AFib. The numbers indicate the number of total peptide spectra identified for each protein. Fibrinogen A $\alpha$ -chain is the most abundant protein amyloidogenic in this sample set, consistent with AFib amyloidosis in each case. To show the presence of mutated proteins in the amyloid plaques, the raw mass spectrometry data files were searched using the human SwissProt database supplemented with A $\alpha$ -chain variants Glu526Val and Phe521Leufs. Consistent with genetic analysis, cases 1-6 contain the tryptic peptide carrying the Glu526Val variant (Row 7, green rectangle), whereas this variant is not present in the case with the Phe521Leufs variant. In contrast, the novel tryptic peptides generated by the frameshift in Phe521Leufs variant are only present in case 7 (Row 17, red rectangle). (B) shows the A $\alpha$ -chain protein coverage in seven cases of AFib amyloidosis. Cases 1-6 carry the Glu526Val variant and case 7 the Phe521Leufs variant. The top line represents the C-terminal sequence of native A $\alpha$ -chain. The amino acid residues of Phe521Leufs (F521 in red) and Glu526Val (E526 in green) are indicated. The first line of rectangles (blue) labeled “WT” represents the coverage of the wild-type A $\alpha$ -chain by the mass spectrometry-based proteomic method used. Two samples (S1 and S2) from four patients are shown. In cases 1-6 (Glu526Val variant), most of the coverage is identical to the wild-type A $\alpha$ -chain except for the tryptic peptide carrying the point mutation (green rectangle) instead of the amino acid present in the wild-type peptide. In case 7 (Phe521Leufs), frameshift leads to a novel sequence indicated by the red rectangle and

amino acid sequence in red letters. No native A $\alpha$ -chain peptides are present after the frameshift mutation, indicating that only the mutant A $\alpha$ -chain is present in amyloid deposits.

**Figure 3. *In silico* studies of human A $\alpha$ -chain amyloidogenic frameshift variants.**

(A) The TANGO aggregation scores of Phe521Leufs variant exhibited a very strong signal for  $\beta$ -sheet aggregation for VLITL at pH 2 (full line) and pH 8 (dotted line) at its C-terminus. (B) PASTA2 predicted that VLITL is likely to stabilize the cross- $\beta$  core of fibrillar aggregates and predicts parallel in-register intermolecular  $\beta$ -sheets for VLITL.

**Figure 4. *In vitro* fibrillogenesis and structural analysis of A $\alpha$ -chain frameshift-derived polypeptides identified in amyloid deposits *in vivo*.**

(A) shows ThT fluorescence assays performed on AFFDTASTGKTFPGFFSPMLGELSVRLSLGAQNLASSQIQRNPVLITLG (red curve) and AFFDTASTGKTFPGFFSPMLGELSVRLSLGAQNLASSQIQRNP\_G (blue curve). Characteristic enhanced ThT fluorescence at 485 nm was only observed for AFFDTASTGKTFPGFFSPMLGELSVRLSLGAQNLASSQIQRNPVLITLG suggesting that this peptide formed amyloid  $\beta$ -sheet structures. In contrast, a spectral red shift at 510 nm was recorded for AFFDTASTGKTFPGFFSPMLGELSVRLSLGAQNLASSQIQRNP\_G, suggesting that it does not form typical amyloid  $\beta$ -sheet structures. (B) Transmission electron micrographs showed that AFFDTASTGKTFPGFFSPMLGELSVRLSLGAQNLASSQIQRNPVLITLG forms fibrillar aggregates and AFFDTASTGKTFPGFFSPMLGELSVRLSLGAQNLASSQIQRNP\_G spherical aggregates. (C) Fibrils formed by AFFDTASTGKTFPGFFSPMLGELSVRLSLGAQNLASSQIQRNPVLITLG exhibited a meridional peak at 4.72 Å, indicating the spacing between  $\beta$ -strands within fibrils associated with an equatorial reflection at 11.50 Å. This microdiffraction pattern confirms the presence of the characteristic amyloid cross- $\beta$  architecture constituted by intermolecular  $\beta$ -sheets with  $\beta$ -strands oriented perpendicular to the fibril axis. (D) presents an extracted radial profile from the 2D pattern shown in (C). The noisy background is due to the small angle used for the profile extraction to avoid the intense peaks from salts in the sample. (E) shows data from ThT fluorescence assays performed on ASSQIQRNPVLITLG (red curve) and ASSQIQRNP\_G (blue curve), revealing that only ASSQIQRNPVLITLG induces enhanced fluorescence at 485 nm and that only the peptide containing VLITL forms aggregates with  $\beta$ -sheet conformation. (F) Transmission electron micrographs showed that ASSQIQRNPVLITLG forms aggregates of fibrillar morphology. (G) shows XRD profiles of ASSQIQRNPVLITLG fibrils displaying the typical “cross- $\beta$ ” microdiffraction pattern of amyloid fibrils with a spacing of 4.75 Å along the meridional direction and a periodicity of 9.90 Å in the equatorial direction. (H) illustrates the *in situ* X-ray microdiffraction pattern from a cut of the pathological kidney specimen of patient II.2 with *in vivo* amyloid fibrils, showing meridional (4.71 Å) and equatorial (10.0 Å) reflections. (I) shows a ThT fluorescence assay of VLITL with increased fluorescence intensity at 485 nm, demonstrating that the dye bound to  $\beta$ -

sheet-enriched amyloid fibrils. (J and K) show transmission electron micrographs of mature VLITL fibrils with ribbon-like structures at different magnifications. Frayed ribbons are observed at the ends of the VLITL twisted fiber structures. The scale bar represents 200 nm. (L) The VLITL fibrils exhibited strong meridional (4.65 Å) and equatorial (10.7 Å) reflections characteristic of a cross-β pattern, confirming their amyloid nature.

**Figure 5. Structural characteristics of AFFDTASTGKTFPGFFSPMLGELSVRLSLGAQNASSQIQRNP\_G assemblies.** (A) shows the morphological features of aggregates. Note that these aggregates are spherical and do not form fibrillar structures, in contrast to amyloid fibrils formed by AFFDTASTGKTFPGFFSPMLGELSVRLSLGAQNASSQIQRNPVLITLG (Fig. 4B). (B) X-ray microdiffraction did not reveal a cross-β microdiffraction pattern, demonstrating that the aggregates are not amyloid.

**Table 1. Summary of FGA variants associated with renal amyloidosis.** Irrespective of the nucleotide position of the FGA deletion/insertion anomalies, all frameshifts truncate at codon 548 and generate similar mutant C-terminal sequences. In the third column of the Table are shown the predicted C-terminal portions of frameshifts: in black are the portion which differs of four/five residues between frameshifts and in blue is the common 15 amino acid sequence, shared by all frameshifts: ASSQIQRNPVLITLG contains the VLITL motif (underlined). All amyloidogenic Aα-chain frameshift variants are listed according to the two nomenclatures. To convert the conventional mature protein amino acid numbering to the HGVS nomenclature, add 19 nucleotides for Aα-chain changes.



Figure 2

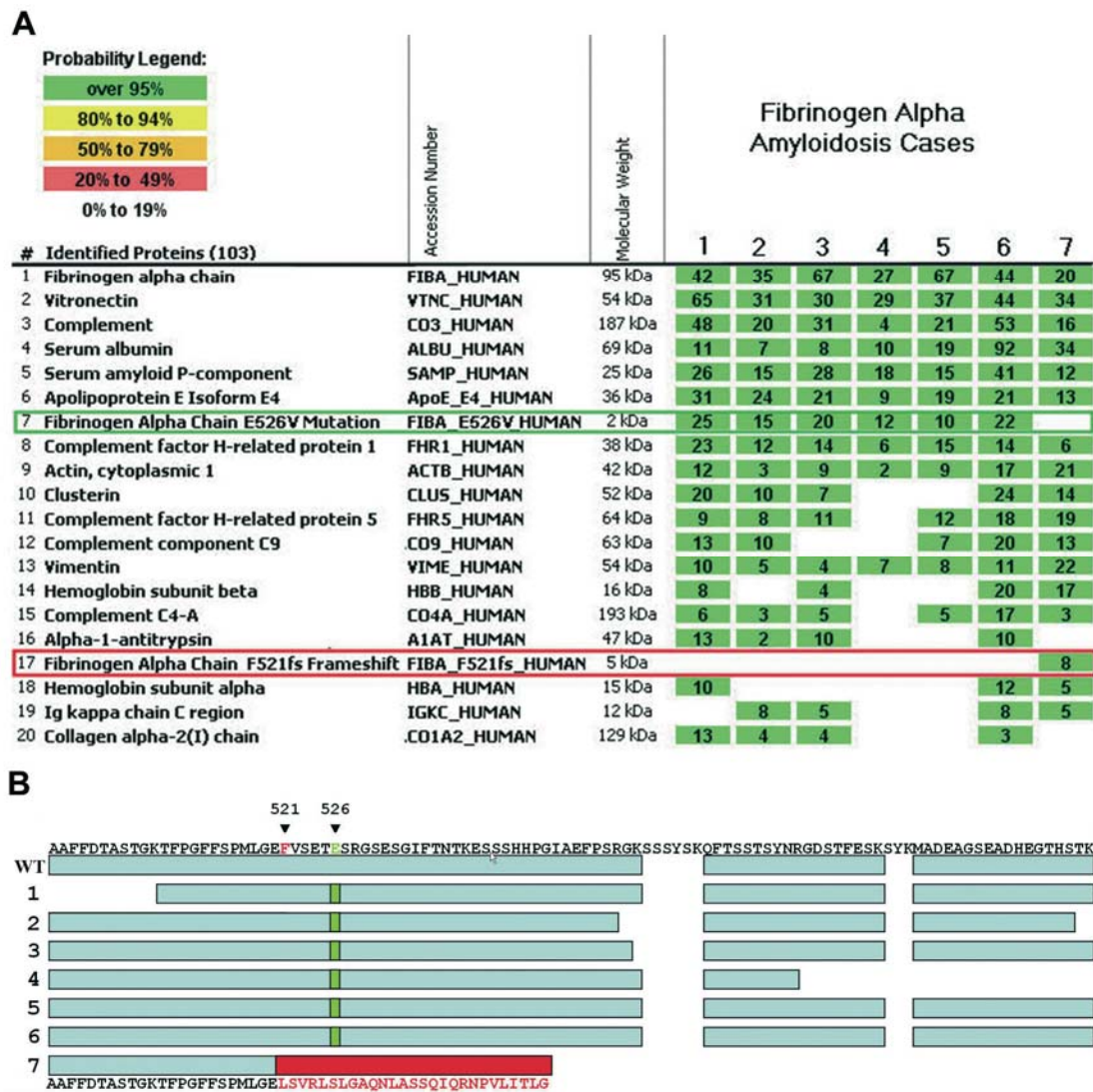


Figure 3

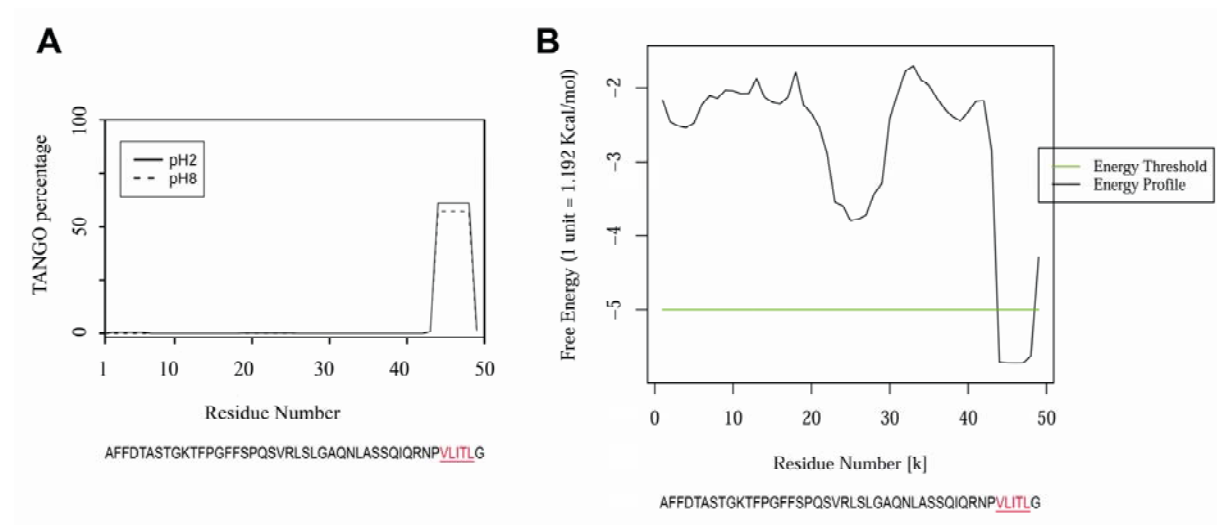


Figure 4

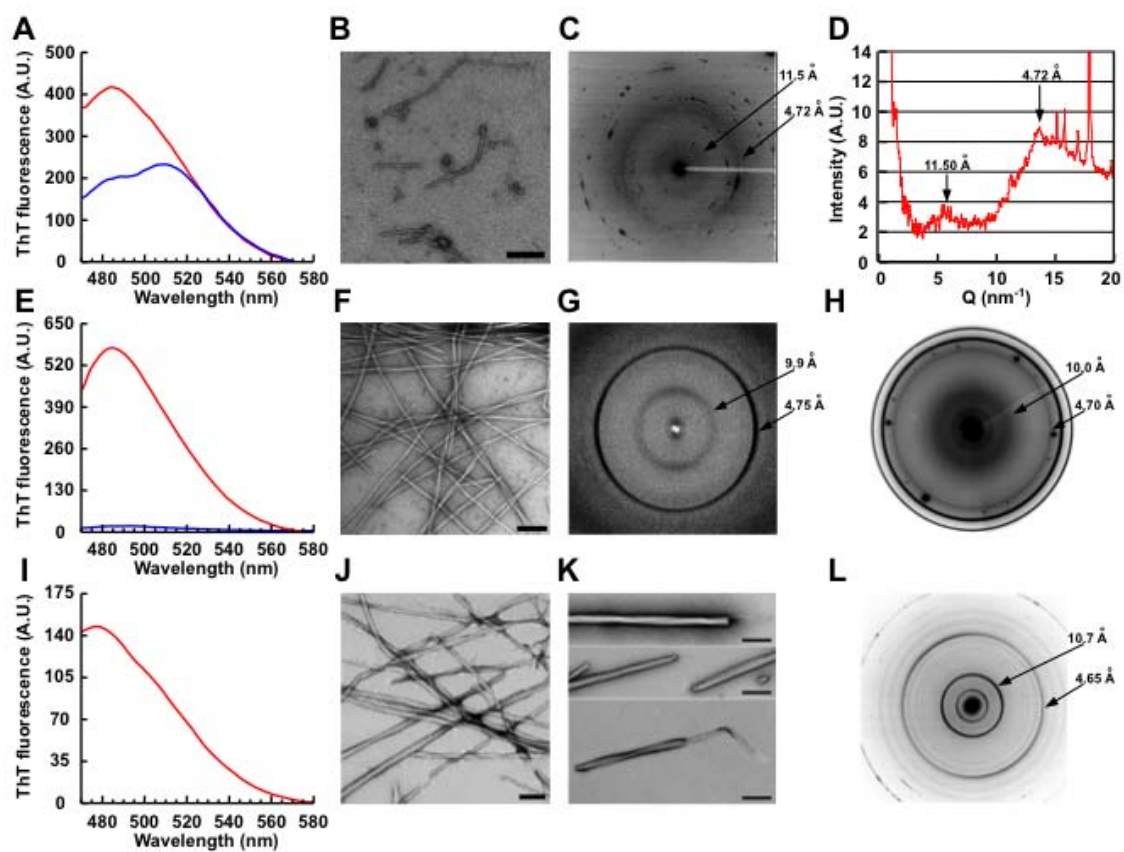


Figure 5

